

Kaempferol Synergistically Enhances Cisplatin-induced Apoptosis and Cell Cycle Arrest in Colon Cancer Cells

Muhammad Haroon, Sun Chul Kang

Department of Biotechnology, Daegu University, Gyeongsan, Korea

Colon cancer remains a significant global health concern, necessitating the continuous exploration of novel therapeutic strategies. Cisplatin is a first-line chemotherapy medication that is frequently used to treat patients for a variety of malignancies, including colon cancer. However, a major obstacle to its clinical usefulness is acquired resistance. This research investigates the synergistic effects of kaempferol, a natural flavonoid with known anti-cancer properties, in combination with cisplatin, in colon cancer cells. Our study employed colon cancer cell lines to evaluate the individual and combined cytotoxic effects of kaempferol and cisplatin. The results demonstrated a notable enhancement in the cytotoxicity of colon cancer cells when treated with a combination of kaempferol and cisplatin compared to individual treatments. This synergistic effect was further characterized by an increase in apoptosis, as evidenced by morphological changes and biochemical markers of apoptosis and cell cycle. The investigations revealed that the combined treatment led to the modulation of key apoptotic pathways, including the upregulation of pro-apoptotic factors and downregulation of anti-apoptotic factors. Additionally, the synergistic effect was associated with the inhibition of cell proliferation and induction of cell cycle arrest. The findings of this study suggest that the combination of kaempferol and cisplatin holds promise as a potent therapeutic strategy for colon cancer treatment, potentially enhancing the efficacy of conventional chemotherapy while minimizing adverse effects. Further in-depth investigations, including *in vivo* studies, are warranted to validate these findings and explore the translational potential of this synergistic approach in clinical settings.

Key Words Flavonol, Cisplatin, Drug synergism, Apoptosis, Cell cycle arrest

INTRODUCTION

The tumor stage of colorectal cancer determines its prognosis. Stage I patients have a 90% 5-year survival rate, compared to 10% for stage IV patients. Even though 60% of patients may have their tumors surgically removed after diagnosis, 20% to 25% of patients can have tumor spread and recurrence following treatment, which can be fatal [1]. Several therapeutic alternatives have emerged. Currently used clinical practice in the management of cancer include targeted treatment, chemotherapy, radiation, and surgical resection [2]. Despite being a crucial strategy for colorectal cancer treatment, chemotherapy's significant side effects and easily developed drug resistance limit its efficacy to a small number of individuals.

Cisplatin, platinum-based chemotherapy, is a commonly used treatment for colorectal cancer [3]. Nevertheless, despite the initial response to cisplatin, most cancer patients

eventually relapse and acquire treatment resistance [4]. Recently, combined chemotherapy is considered a superior treatment strategy [5]. Therefore, there is an urgent need to find efficient chemosensitizers that can boost anticancer medication efficacy while overcoming adverse effects and multidrug resistance.

Cancer cells naturally produce more reactive oxygen species (ROS) than normal cells [6]. The elevation of ROS is crucial for the initiation and progression of cancer. On the other hand, excess production of ROS may be hazardous and increase the susceptibility of cancer cells to more oxidative stress induced by external factors [7]. It has been reported that oxidative stress can cause cell death through several mechanisms, including mitochondrial cascade and endoplasmic reticulum (ER) stress [8]. As a result, regulating ROS levels allows for the selective killing of cancer cells and is linked to the anti-tumor properties of several therapeutic drugs, such as piperlongumine, disulfiram, and auranofin [9].

Received July 26, 2024, Revised September 19, 2024, Accepted September 19, 2024, Published on September 30, 2024
Correspondence to Sun Chul Kang, E-mail: sockang@daegu.ac.kr, https://orcid.org/0000-0002-1580-3266



This is an Open Access article distributed under the terms of the Creative Commons Attribution Non-Commercial License, which permits unrestricted non-commercial use, distribution, and reproduction in any medium, provided the original work is properly cited.

Copyright © 2024 Korean Society of Cancer Prevention

Natural substances originating from plants have been utilized to treat malignancies of various types [10]. Kaempferol, (3,5,7-trihydroxy-2-(4-hydroxyphenyl)-4H-1-benzopyran-4 one), is a naturally occurring flavonoid in a wide variety of vegetables and fruits, such as broccoli, tomatoes, onions, red fruits, grapes and tea [11]. This polyphenol has antioxidant, inflammatory and antineoplastic effects [12]. Additionally, kaempferol can affect a variety of cellular pathways that disrupt the survival or regulation of some cancer cells [13].

The current study aimed to determine whether kaempferol had synergistic effect with cisplatin on inhibiting colon cancer cell growth through induction of apoptosis. Kaempferol enhanced the induction of cell cycle arrest and apoptosis, which led to a synergistic impact. The analyses revealed that kaempferol, as a ROS inducer, may significantly increase the death of colon cancer cells caused by cisplatin *in vitro* by inducing a ROS-mediated pathway.

MATERIALS AND METHODS

Materials

RPMI-1640, Dulbecco's Modified Eagle Medium (DMEM), Rhodamine-123, dichlorodihydrofluorescein diacetate (H₂D-CFDA), DAPI, 3-(4,5-dimethylthiazol-2-yl)-2,5-diphenyltetrazolium bromide (MTT) and dimethylsulfoxide (DMSO) were purchased from Sigma-Aldrich. FBS was from Gibco. A list of the antibodies used in the study is provided in the Table S1. All other chemicals, unless otherwise mentioned, were purchased from Sigma-Aldrich.

Cell culture and *in vitro* assays

In RPMI-1640 media, human colon cancer HCT-15 cells and HCT-116 cells (ATCC) (KCLB) were cultivated. DMEM medium was used to culture the human skin keratinocytes (HaCaT) (KCLB) and the human embryonic kidney (HEK-293) cell line (ATCC). Cells were kept in a 5% CO₂ incubator at 37°C and both media were supplemented with 10% FBS (Gibco) and 1% penicillin-streptomycin (Gibco). HCT-15 and HCT-116 cells were grown in 3 mm cell culture plates (SPL) with a cell number of 1.0×10^5 cells/well for various experiments.

Cell viability measurements

The MTT assay was used for the assessment of cell viability. Briefly, HCT-15, HCT-116, HaCaT, and HEK-293 cells were seeded at a density of 1.0×10^4 cells/well in a 96-well flat-bottom microtiter plate and allowed to adhere and proliferate for 24 hours at 37°C and 5% CO₂. Cells were subsequently treated with various concentrations of kaempferol (10, 30, and 50 μM) and cisplatin (1, 5, and 10 μM) or their combination. HaCaT and HEK-293 cells were treated with kaempferol (50 μM) and cisplatin (10 μM) or their combination followed by incubation for 48 hours at 37°C and 5% CO₂. The plates were then incubated for 4 hours at 37°C after the wells were

replaced with 50 μL of fresh media along with 50 μL of the MTT working solution (2.5 mg/mL dissolved in PBS). Following aspiration of the medium, 150 μL of DMSO was added to each well to solubilize the produced formazan crystals. Using an ELISA plate reader, the amount of purple color produced by the formazan crystals' dissolution was measured at 540 nm.

Clonogenic assay

We conducted experiments to assess cell proliferation and colony-forming assay. Briefly, 6-well cell culture plates (BD Falcon) were used to seed HCT-15 and HCT-116 cells at a density of 1.0×10^4 cells/well in RPMI-1640 media. Colon cancer cells, were subsequently treated with kaempferol (50 μM) and cisplatin (10 μM) or their combination. After the incubation, fixation of the cells was carried out with 4% (w/v) formaldehyde, followed by staining with 0.1% (w/v) crystal violet solution, and then photographs were taken.

Bromodeoxyuridine cell proliferation assay

The bromodeoxyuridine (BrdU) assay was conducted with a commercially available BrdU labelling and detection kit (Abcam; ab126556), following the instructions provided by the manufacturer. Briefly, 96-well cell culture plates (BD Falcon) were used to seed HCT-15 and HCT-116 cells at a density of 1.0×10^5 cells/well in RPMI-1640 media. Cells were subsequently treated with kaempferol (50 μM) and cisplatin (10 μM) or their combination for 48 hours. The BrdU uptake was measured according to steps in the kit manual and the absorbance was measured using an ELISA microtiter plate reader at 450/540 nm.

Cellular senescence assay (senescence-associated β-galactosidase activity)

Detecting SA-β-Gal activity using a fluorometric substrate is an effective way to assess cellular senescence (96-Well cellular senescence assay kit, CBA-231, Cell Biolabs, Inc.) [14]. Briefly, 96-well cell culture plates (BD Falcon) were used to seed HCT-15 and HCT-116 cells at a density of 1.0×10^5 cells/well in RPMI-1640 media. Cells were subsequently treated with kaempferol (50 μM) and cisplatin (10 μM) or their combination for 48 hours. The fluorescence was measured at 360 nm (excitation)/465 nm (emission).

Estimation of intracellular ROS generation

HCT-15 and HCT-116 cells were cultured in 12-well cell culture plates at a density of 1.0×10^6 cells/well in 2 mL RPMI media. The cells were subsequently treated with kaempferol (50 μM) and cisplatin (10 μM) or their combination. After treatment, cells were washed with PBS before addition of 10 μM of H₂DCFDA dye, a peroxide-sensitive fluorescent probe. After incubation for 30 minutes. ROS production was detected with a fluorescence microscope. To measure the production of superoxide in mitochondria, the cells were stained with 5

μM MitoSOXTM Red (Thermo Fisher Scientific). The staining of cells was observed under an inverted fluorescence microscope.

Estimation of nitric oxide generation

Cells were treated with kaempferol (50 μM) and cisplatin (10 μM) or their combination. Griess reagent was added to the cell homogenate, followed by incubation for 15 minutes at room temperature in the dark and the absorbance at 540 nm was measured. Using sodium nitrite as a standard, the amount of NO was estimated against the standard curve.

Determination of mitochondrial membrane potential

Briefly, 1.0×10^6 HCT-15 and HCT-116 cells/well were cultured in 12-well cell culture plates. Following this, cells were treated with kaempferol (50 μM) and cisplatin (10 μM) or their combination. After washing the cells with PBS, 10 $\mu\text{M}/\text{mL}$ Rh-123 dye was added, and the cells were incubated for 30 minutes. Following a PBS rinse, fluorescence microscopy at 20 \times magnification was used to determine the degree of mitochondrial membrane damage.

Quantitative analysis of ATP

Cells were treated with kaempferol (50 μM) and cisplatin (10 μM) or their combination against HCT-15 and HCT-116 cells in a 96-well plate at a density of 1.0×10^4 cells/well. The measurement of ATP was carried out according to the instructions provided by the manufacturer (ATP Bioluminescent Assay Kit; FLAA, Sigma-Aldrich).

Determination of chromatin condensation by DAPI

Briefly, the cells were cultured in 12-well cell culture plates at a density of 1.0×10^6 cells/well in 2 mL RPMI media. Cells were treated with kaempferol (50 μM) and cisplatin (10 μM) or their combination and then incubated for 48 hours. Following a PBS wash, treated cells were exposed to 1 $\mu\text{g}/\text{mL}$ DAPI and incubated for 30 minutes at 37°C. The cells were rinsed with PBS and the cells were photographed using a fluorescence microscope at 20 \times magnification.

Estimation of lactate dehydrogenase release

Cells were treated with kaempferol (50 μM) and cisplatin (10 μM) or their combination. Lactate dehydrogenase (LDH) leakage into the culture medium from cells was measured using an LDH assay kit (Sigma-Aldrich) to determine the integrity of the plasma membrane.

Western blot analysis

Cells were treated with kaempferol (50 μM) and cisplatin (10 μM) or their combination. Following incubation, cell lysis was carried out using RIPA buffer. SDS-polyacrylamide gel electrophoresis was conducted using 100 μg of protein per lane.

On a polyvinylidene difluoride (PVDF) membrane, proteins were transferred. Non-specific proteins were inhibited by incubating the PVDF membrane in 3% to 5% BSA for 2 hours at room temperature. The membrane was then treated with a primary antibody, followed by an appropriate HRP-conjugated secondary antibody. The PVDF-membrane blots were then using the enhanced chemiluminescence reagent, which was obtained from Amersham Biosciences Inc. Using ImageJ software, version 1.8.0, the intensity of protein bands was calculated.

Gene silencing with p53 small interfering RNA

HCT 116 cells were transfected with small interfering RNA (siRNA) specific to p53 or scrambled (SCR) siRNA as a control. The siRNA sequences were acquired from Integrated DNA Technologies (IDT, Inc.). The p53 siRNA sequence employed was (sense) 5'-GACUCCAGUGGUAUUCUAC-3' and (antisense) 5' GUAGAUUACCACUGGAGUC-3'. The transfections were conducted utilizing lipofectamine 3000 (Invitrogen). For each well, a total of 5 pmol of either p53-siRNA or SCR-siRNA was mixed with RPMI serum-reduced medium (Gibco). Lipofectamine-3000 reagent was mixed with RPMI.

Flow cytometry-based apoptosis detection

The fluorescence activated cell sorting (FACS) analysis was conducted using a FITC Annexin V Apoptosis Detection Kit I (BD Pharmingen). Cells were treated with kaempferol (50 μM) and cisplatin (10 μM) or their combination. The cells were examined using a BD FACS VerseTM cell analyzer. FlowJo 7.6.1 Software was used to analyze the results.

Cell-cycle analysis

Flow cytometry was carried out for the cell-cycle profiling [15]. The cells were exposed to kaempferol (50 μM) and cisplatin (10 μM) alone or in combination. Cells were harvested by using a 0.05% trypsin-EDTA solution after treatment. Cell pellets were redissolved in 0.1 mL of 1 \times PBS, and 2 mL of RNase solution (100 mg/mL), and the suspension was incubated at 37°C for an hour. Propidium iodide (PI) solution (50 $\mu\text{g}/\text{mL}$) was then added, and the mixture was gently vortexed. And the contents were examined using BD FACS VerseTM cell analyzer. FlowJo 7.6.1 Software was used to analyze the results.

Statistical analysis

The mean \pm standard deviation of 3 independent experiments was used to represent the data. Data were examined using one-way analysis of variance (ANOVA) and Student's t-tests in GraphPad Prism Software for the statistical comparisons (version 8.0.1).

RESULTS AND DISCUSSION

Co-treatment of kaempferol and cisplatin synergistically enhances cell death in colon cancer cells

The synergistic effect of cisplatin with natural apoptosis inducers was determined as reported previously [16]. Our results

demonstrate a remarkable synergy between cisplatin and kaempferol across a range of concentrations in colon cancer cells.

Cells treated with kaempferol (10 and 30 μM) had slightly decreased the HCT-15 and HCT-116 cell proliferation, while significant effects were observed at the highest concentration (50 μM) as compared to the control cells. The cisplatin con-

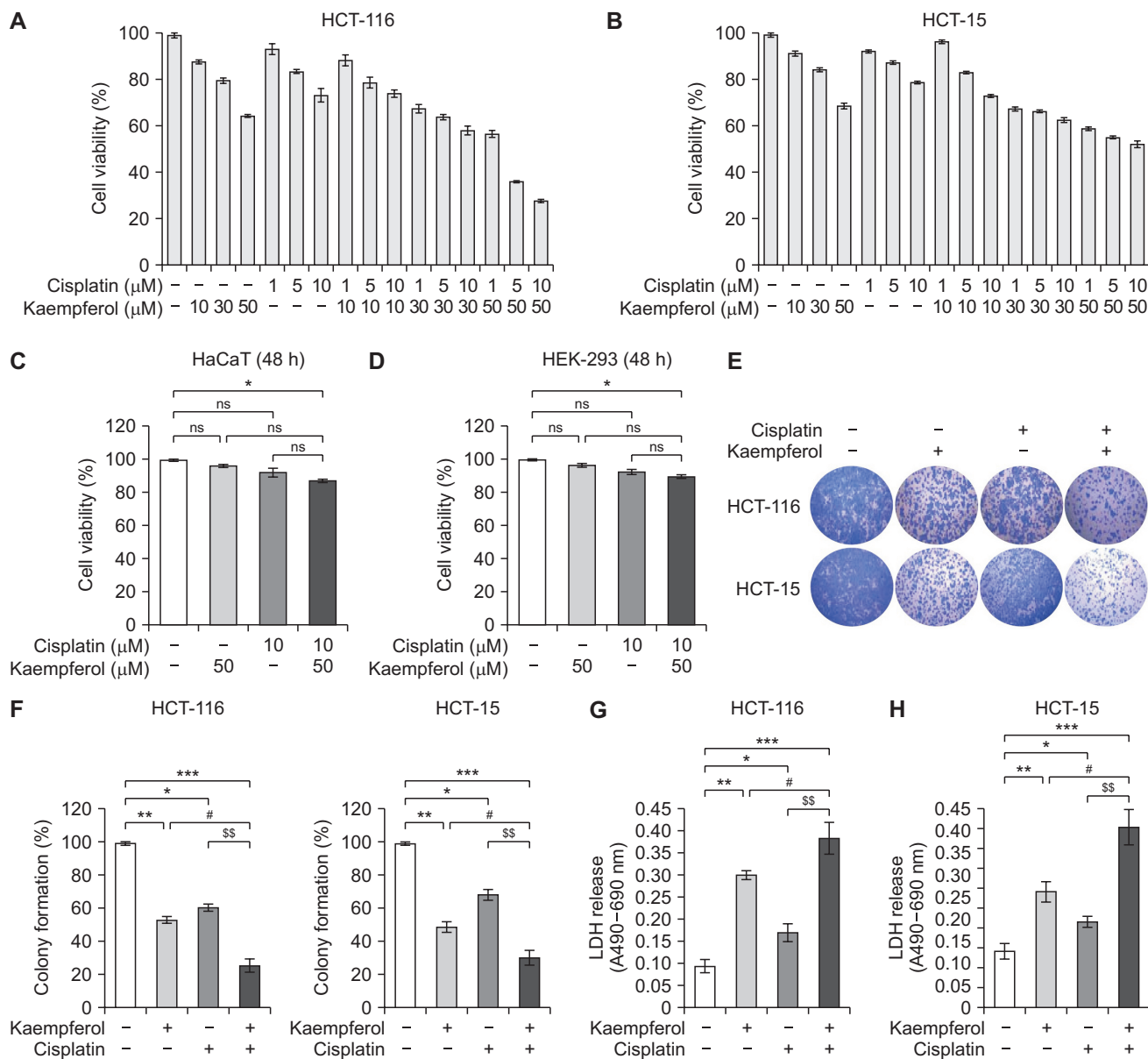


Figure 1. Assessment of cell viability for kaempferol alone or in combination with cisplatin against human colon cancer and normal cell lines. (A) and (B) The graphs represent the percentage of viable HCT-116 and HCT-15 cells after treatment with kaempferol (10, 30, and 50 μM) and cisplatin (1, 5, and 10 μM) and their combination after 48 hours. (C) and (D) the graphs represent cytotoxicity assessment for kaempferol and cisplatin alone or in combination for 48 hours against human keratinocytes (HaCaT) and human embryonic kidney-293 (HEK-293) cell lines. (E) Effects of kaempferol and cisplatin alone or in combination were evaluated against the colony formation ability of HCT-116 and HCT-15 colon cancer cell lines. (F) The graphs represent the relative colony formation ability of HCT-116 and HCT-15. (G) and (H) cell viability in colon cancer was also determined by the LDH release assay for cells treated with kaempferol and cisplatin alone or in combination. The data are represented as the mean \pm standard deviation. * $P < 0.05$, ** $P < 0.01$, and *** $P < 0.001$ for comparison between control and treated cells, whereas # $P < 0.05$ for comparison between kaempferol alone and combination and $^{ss}P < 0.01$ for comparison between cisplatin only and combine treatment. ns, not significant.

centration (10 μM) was selected based on the cytotoxicity assessment by using various concentrations of the compound in normal cells. The MTT results are shown in Figure 1A and 1B.

The cytotoxicity evaluation of the cisplatin and kaempferol, alone or in combination was evaluated in normal cell lines such as HEK-293 and HaCAT cells. No significant reduction in the proliferation was observed in these normal cells treated with a combination of kaempferol (50 μM) and cisplatin (10 μM) (Fig. 1C and 1D).

For the confirmation of these results, we investigated the colony formation ability. The kaempferol (50 μM) and cisplatin (10 μM) co-treated cells dramatically decreased the number of colonies (Fig. 1E and 1F). When the cell membrane is damaged, the enzyme LDH is released [17]. LDH release at 48 hours after exposure to kaempferol and cisplatin alone or in combination are shown in Figure 1G and 1H in which there was a significant increase in the LDH release in kaempferol and cisplatin co-treated cells.

The MTT assay revealed that a combination of kaemp-

ferol (50 μM) and cisplatin (10 μM) significantly ($P < 0.001$) increased the rate of cell death in both cell lines. Patterns of synergism were observed in HCT-15 cells and HCT-116 cells, and the cell viability was determined to be $50.6\% \pm 3\%$ ($P < 0.001$) and $26.9\% \pm 2.5\%$ ($P < 0.001$), respectively. The synergism evaluation for the cisplatin and kaempferol was carried out with Synergy Finder 3.0 [18], as shown in Figure 2.

Kaempferol and cisplatin enhance cellular senescence in colon cancer cells

The morphological study of both HCT-15 and HCT-116 cell lines showed noticeable changes that are typical of senescent cells, such as larger and flatter forms with increased granularity and the changes were more prominent in the group that received the co-treatment indicating a synergistic interaction (Fig. 3A). These alterations are the hallmark of cellular senescence-like phenotype [19]. The BrdU uptake assay is an essential method for quantifying cell proliferation and DNA synthesis, and it has a significant role in demon-

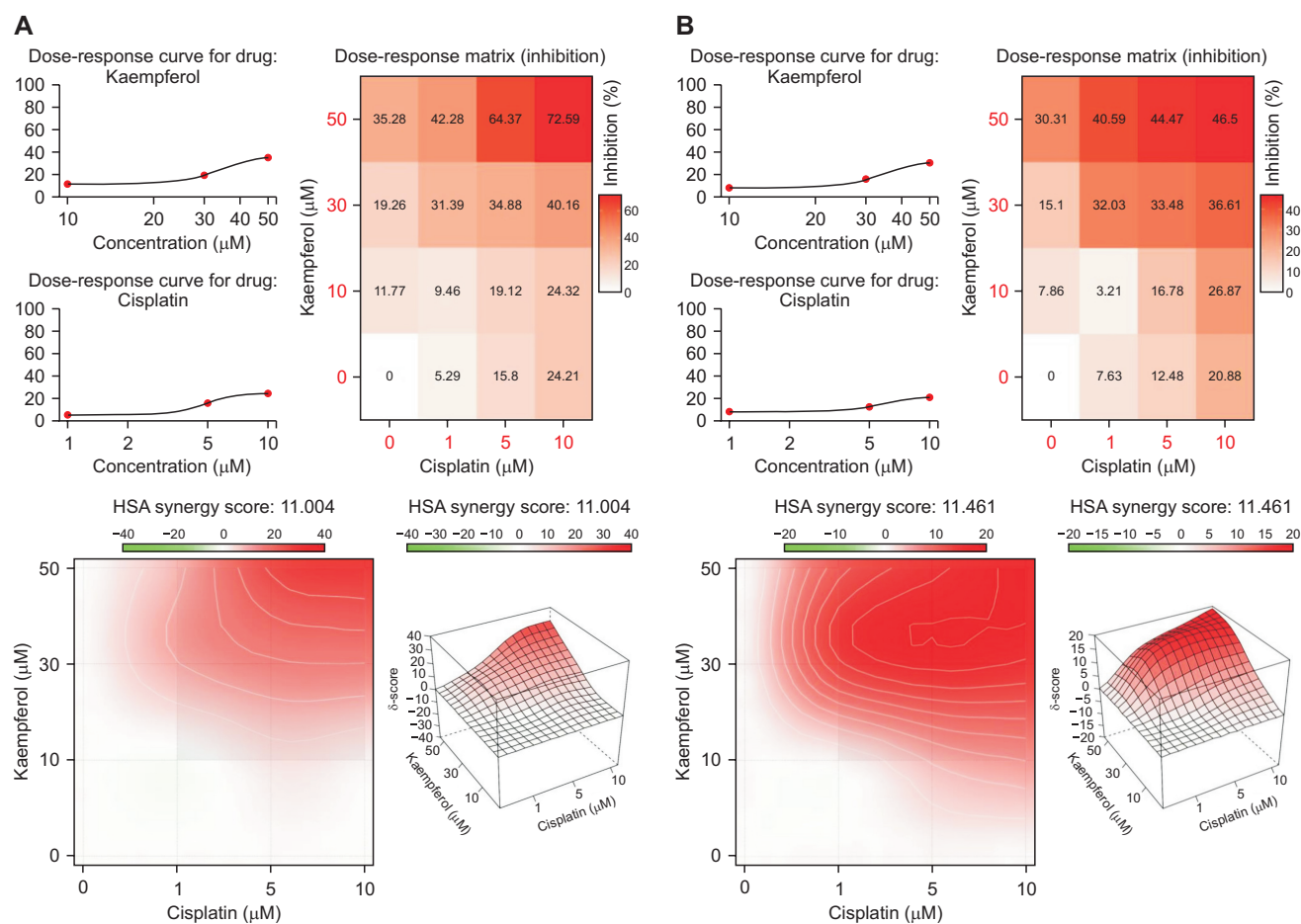


Figure 2. Synergistic activity for kaempferol and cisplatin against colon cancer HCT-15 and HCT-116 cells. Evaluation of the synergistic potential of kaempferol and cisplatin co-treatment in colon cancer cells (A) HCT-116 and (B) HCT-15. Single-agent dose-response curves for each drug and their combinatory effect were assessed through the combination index (CI) plot, highlighting synergy (HSA synergy score > 10). Heatmap displaying the CI values across different drug concentrations.

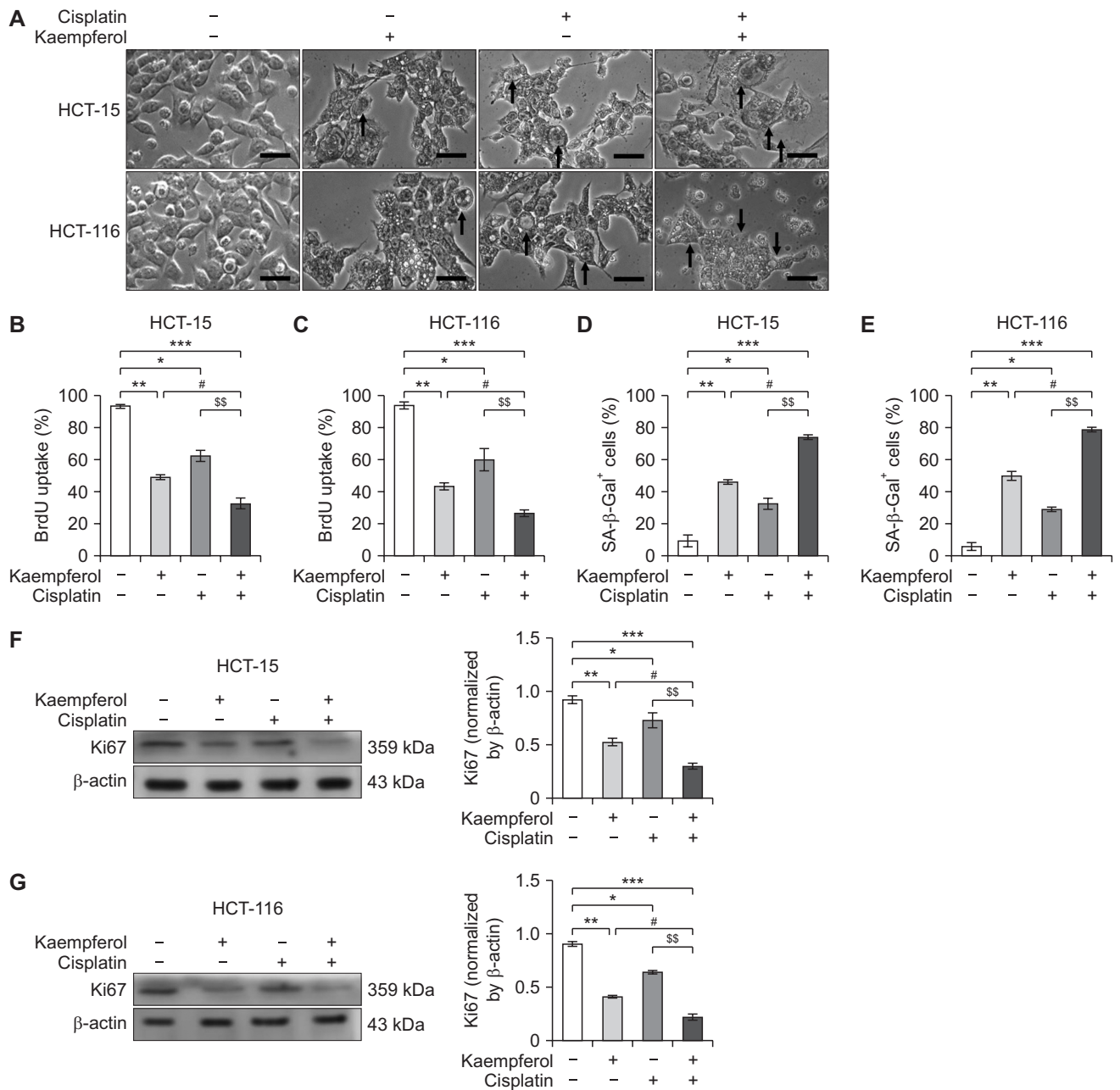


Figure 3. Kaempferol and cisplatin co-treatment induced cellular senescence in human colon cancer HCT-15 and HCT-116 cells. (A) Morphological images depict cellular alterations associated with senescence, including flattened and enlarged cell morphology (Magnification 20× and scale bar 100 μm). (B, C) The BrdU assay was performed to assess cell proliferation. (D, E) The senescence-associated β-galactosidase (SA-β-Gal) assay was used to assess the cellular senescence. (F, G) Ki67 protein expression analysis was carried out to evaluate cell proliferation status. The relative protein expression intensity was analyzed with ImageJ software. The data are represented as the mean ± standard deviation. **P* < 0.05, ***P* < 0.01, and ****P* < 0.001 for comparison between control and treated cells, whereas #*P* < 0.05 for comparison between kaempferol alone and combination and ^{ss}*P* < 0.01 for comparison between cisplatin only and combine treatment.

strating cellular senescence [20]. There was a significant decline in BrdU incorporation in cells co-treated with kaempferol and cisplatin in both cell lines (Fig. 3B and 3C). The SA-β-Gal assay is a commonly used technique for identifying cellular senescence [21]. The result showed a notable rise in the percentage of SA-β-Gal-positive cells in the co-treatment group

compared to the other treatment groups (Fig. 3D and 3E). In addition, the cells co-treated with both kaempferol and cisplatin showed a significant decrease in Ki67 expression in both cell lines (Fig. 3F and 3G). Ki67 is a widely known indicator of cell proliferation. It is present during all the active stages of the cell cycle (G1, S, G2, and mitosis) but its expression is

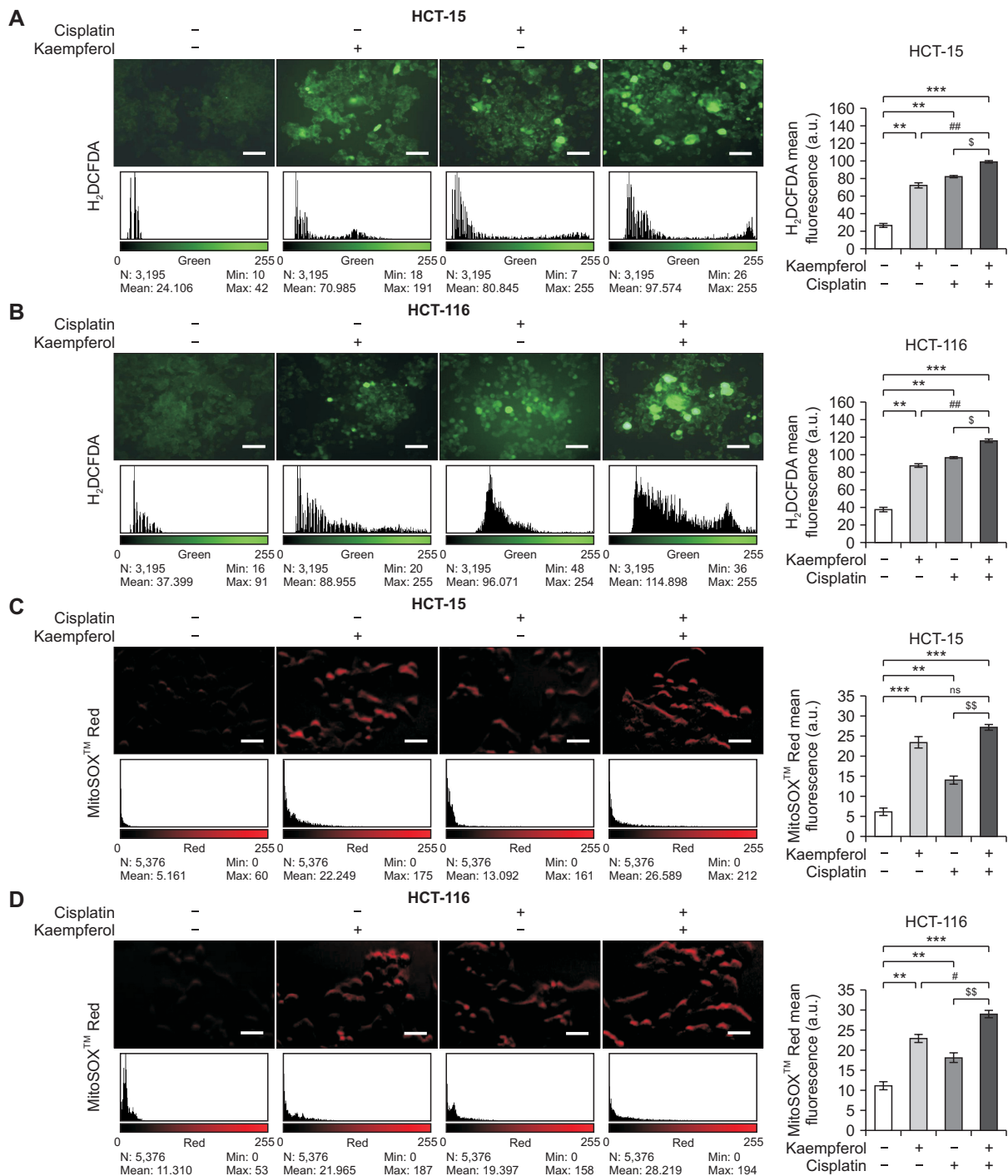


Figure 4. Kaempferol and cisplatin co-treatment induced oxidative stress-mediated inflammatory response in human colon cancer HCT-15 and HCT-116 cells. Colon cancer cells treated with kaempferol, and cisplatin combination promotes changes in reactive oxygen species (ROS) production which is observed by alterations in fluorescence observed via different staining. (A, B) Representative fluorescent microscopy images of HCT-15 and HCT-116 colon cancer cells stained with H₂DCFDA. (C, D) Visualization of mitochondrial ROS was carried out with MitoSOXTM Red staining in HCT-15 and HCT-116 cells. Scale bar of images 100 μ m. The graphs represent the relative fluorescence intensity of the cells treated with kaempferol and cisplatin co-treatment as compared to control. (E) Kaempferol and cisplatin co-treatment further increased the level of nitric oxide production in cells. (F) HCT-15 and (G) HCT-116; kaempferol and cisplatin combine treated cells altered the redox signaling. Quantification of H₂DCFDA, MitoSOXTM Red fluorescence intensity and relative protein expression intensity were analyzed with ImageJ software. The data are represented as the mean \pm standard deviation. * $P < 0.05$, ** $P < 0.01$, and *** $P < 0.001$ for comparison between control and treated cells, whereas # $P < 0.05$, ## $P < 0.01$, and for comparison between kaempferol alone and combination and $^{\$}P < 0.05$, $^{\$\$}P < 0.01$ for comparison between cisplatin only and combine treatment. ns, not significant.

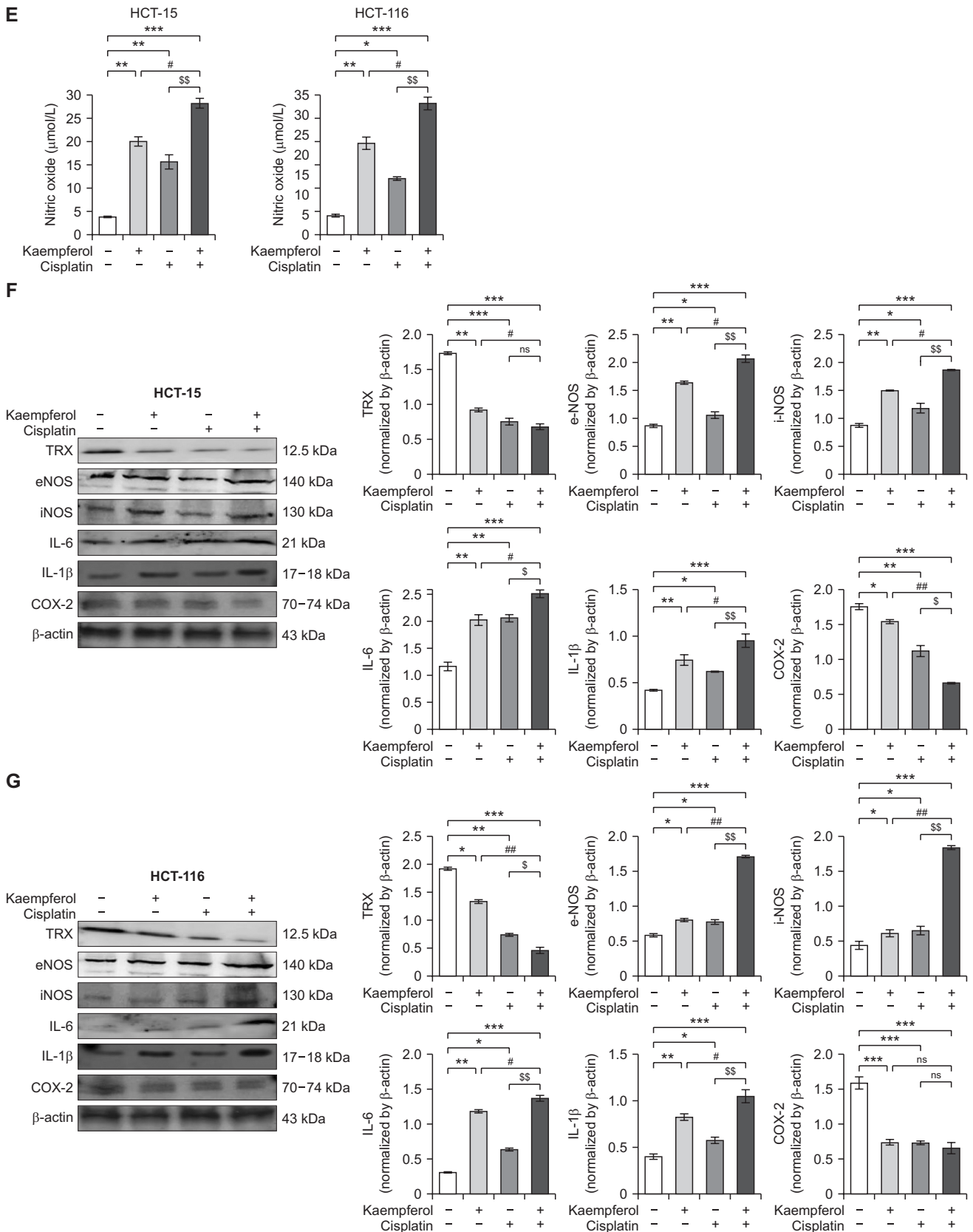


Figure 4. Continued.

reduced in the resting (quiescent) phase (G0) [22].

Synergistic action of kaempferol and cisplatin modulates oxidative stress and inflammatory response

Endogenous free radicals can lead to genotoxic stress, which leads to DNA damage and the start of numerous cell-fate decision-making pathways [23]. The synergistic effect of kaempferol and cisplatin co-treatment ($P < 0.001$) induces a high level of ROS generation as compared to the control group in both cell lines (Fig. 4A and 4B).

MitoSOX™ labelling was carried out to evaluate the generation of mitochondrial ROS. The co-treatment of kaempferol and cisplatin led to the more pronounced MitoSOX™ fluorescence intensity in both cell lines (Fig. 4C and 4D).

The production of molecules like NO, which is the result of cellular senescence, is also severely influenced by chemotherapeutic agents [24]. Additionally, NO synthesis and ROS synthesis together contribute to oxidative stress [25,26]. We examined the NO content of cells treated with kaempferol and cisplatin alone or in combination. As shown in Figure 4E. Kaempferol and cisplatin co-treatment significantly increased the NO production in HCT-15 and HCT-116 cells as compared to other groups.

Furthermore, by analyzing the expression of proteins involved in redox signalling, the condition of oxidative stress was verified at the molecular level. As seen in Figure 4F and 4G, kaempferol and cisplatin combination significantly reduced the TRX protein expression in HCT-15 and HCT-116 cells compared to control. The redox regulation was further supported by the analysis of e-NOS and i-NOS protein expression. Combined treatment significantly increased the expression of i-NOS and e-NOS in both HCT-15 and HCT-116 cells.

Further, we also observed the higher expression of interleukin-6 (IL-6), and IL-1 β which has a role in the regulation of redox balance by regulating the production of NO and other antioxidant enzymes [27]. Kaempferol and cisplatin combined treatment further increased the expression of IL-6, and IL-1 β in both cancer cell lines (Fig. 4F and 4G). COX-2 is an enzyme which causes the conversion of arachidonic acid into prostaglandins, which are lipid mediators implicated in fever, pain, and inflammation [28]. In cells co-treated with kaempferol and cisplatin significantly reduced the expression of COX-2.

These findings suggest that cells with kaempferol, and cisplatin co-treatment lose their antioxidant capacity, which may prevent the preservation of redox state equilibrium [29]. It has been well-recognized that inflammation plays a crucial role in the development of cellular senescence [27].

Impact of kaempferol and cisplatin co-treatment on mitochondrial membrane potential

The mitochondrial membrane's gradient electrochemical po-

tential structure is crucial for the storage of freshly produced ATP. According to several observations, oxidative stress changes the permeability of the mitochondrial membrane [30]. By Rh-123 staining, we could see that the kaempferol and cisplatin co-treatment markedly interfered with the mitochondrial membrane integrity ($\Delta\Psi_m$) of HCT-15 and HCT-116 cells (Fig. 5A). The findings demonstrate a notable reduction of green fluorescence following kaempferol and cisplatin co-treatment (Fig. 5B). To assess the functioning and condition of mitochondria, cells were stained with MitoTracker™ Deep Red (Invitrogen). The decrease in mitochondrial function and damage to mitochondria suggests that the co-treatment has a synergistic effect on impairing the integrity of mitochondria in colon cancer cells (Figure S1).

Alterations in the homeostasis of the mitochondria specifically remove the functioning of the mitochondria, which further causes the unintended loss of cell viability by activating the machinery for programmed cell death [31]. Anticancer drugs frequently target cellular mechanisms such as glycolysis, oxidative phosphorylation, and mitochondrial activity which are essential for the generation of ATP. The reduction of ATP can contribute to cellular stress and ultimately result in cell death [32]. In the current study, we measured the ATP levels in the cells. As shown in Figure 5C, kaempferol and cisplatin co-treatment ($P < 0.001$) apparently lowered ATP to a greater extent than did the individual treatments.

Kaempferol and cisplatin co-treatment significantly enhances DNA damage response

Extended activation of DDR, caused by continuous exposure to ROS and NO, can disturb the regular progression of the cell cycle, resulting in either growth inhibition or apoptosis. In the context of cancer, the prolonged activation of DDR mechanisms can contribute to the advancement of tumors by causing genetic instability and abnormal cell proliferation. This highlights the important relationship between DDR, oxidative stress, and cellular growth [33,34]. DNA damage can be detected by analyzing the fragmentation patterns of DNA taken from treated cells using electrophoresis [35]. The treatment of HCT-15 and HCT-116 colon cancer cells with cisplatin and kaempferol in combination resulted in substantial DNA fragmentation (Fig. 6A).

Further, the DDR was evaluated at the molecular level by measuring the expression level of various protein markers involved in DNA damage repair and response. Expression of γ -H2AX, which is the phosphorylated version of histone H2AX, serves as an indicator DDR activation [36,37]. The high expression of γ -H2AX protein is an indication of double strands break (DSB) mediated DDR [38]. A more prominent in the expression of γ -H2AX in the kaempferol and cisplatin co-treated cells as compared to the other groups (Fig. 6B and 6C).

In the DNA repair system following the kaempferol and cisplatin treatment, the expression of PARP/cleaved-PARP was

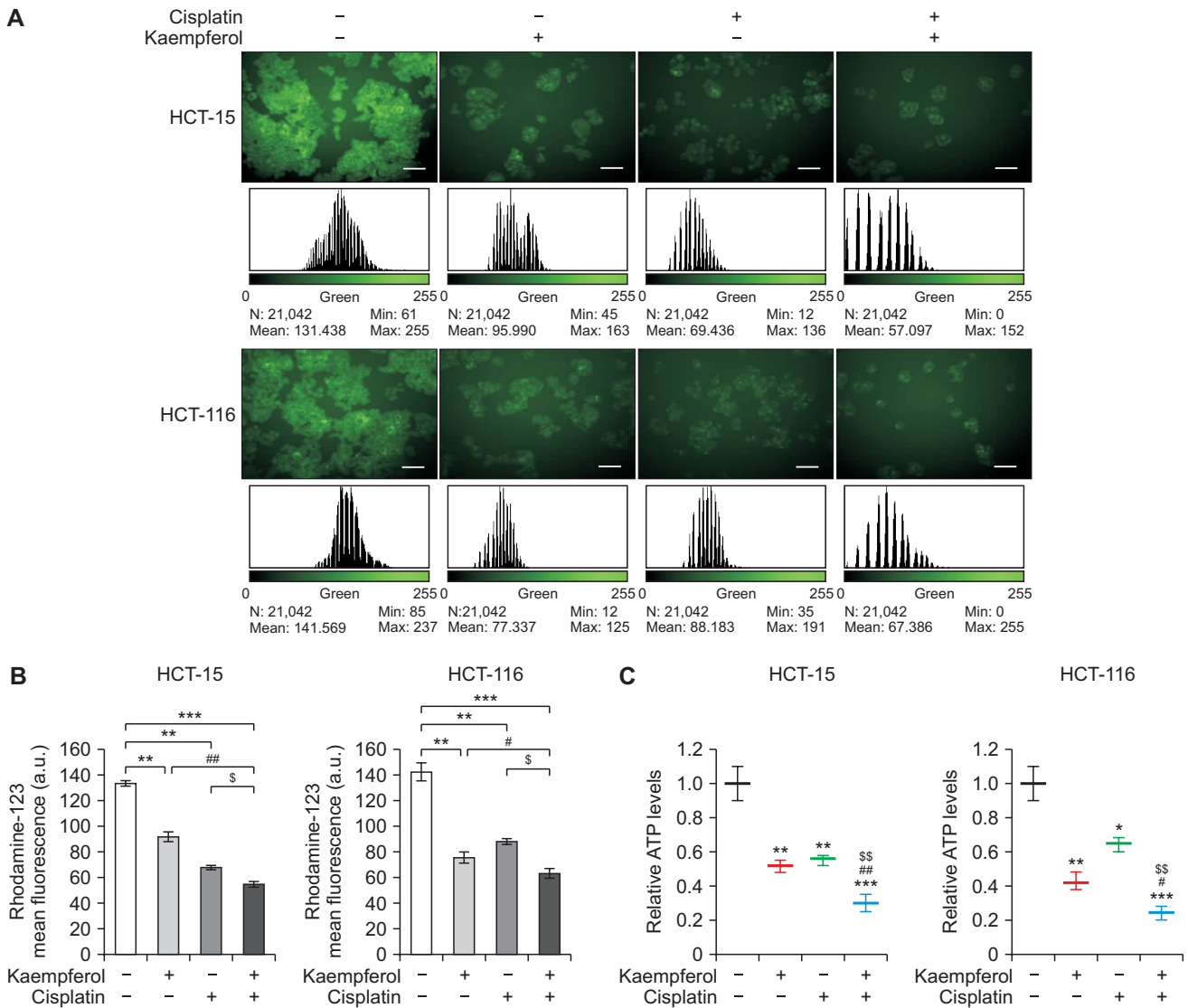


Figure 5. Effects of kasmperol and cisplatin co-treatment mitochondrial membrane potential and ATP synthesis. (A) Representative fluorescent microscopy image of treated colon cancer cells stained with rhodamine 123 (magnification 20x and scale bar 100 μm). (B) The graph represents the change in the relative fluorescence intensity in the cells treated with either kaempferol, cisplatin or their combination. (C) The ATP level was determined in colon cancer cells following kaempferol and cisplatin or their combination treatment. The quantification of rhodamine-123 fluorescence intensity was carried out with ImageJ software. The data are represented as the mean ± standard deviation. **P* < 0.05, ***P* < 0.01, and ****P* < 0.001 for comparison between control and treated cells, whereas #*P* < 0.05, ##*P* < 0.01 for comparison between kaempferol alone and combination and \$*P* < 0.05, \$\$*P* < 0.01 for comparison between cisplatin only and combine treatment.

also analyzed and a significant increase in the expression of cleaved-PARP was observed in the kaempferol and cisplatin co-treated HCT-15 and HCT-116 cells. Additionally, we observed a significant decrease in the expression of ERCC-1 in the kaempferol and cisplatin co-treatment group in both cell lines. ERCC-1 is critically important in the DNA damage repair process [39]. The telomerase reverse transcriptase (hTERT) plays a crucial role in cancer cells by preserving the length of telomeres, which allows for uninterrupted cell division and prevents the aging of cells [40,41]. The combined administration leads to a considerable decrease in hTERT

expression in both cell lines. Conclusively rigorous analysis of the protein expression implicated in the DNA damage and repair event shows that kaempferol and cisplatin co-treatment effectively activates the DNA damage pathway and inhibits the DNA repair system.

Kaempferol enhances the effects of cisplatin to activate the apoptotic pathway

We performed flow cytometry for the detection of the cell population in early apoptosis, late apoptosis and necrosis (Fig. 7A). Q4 represented the percentage of live cells with 89.3%

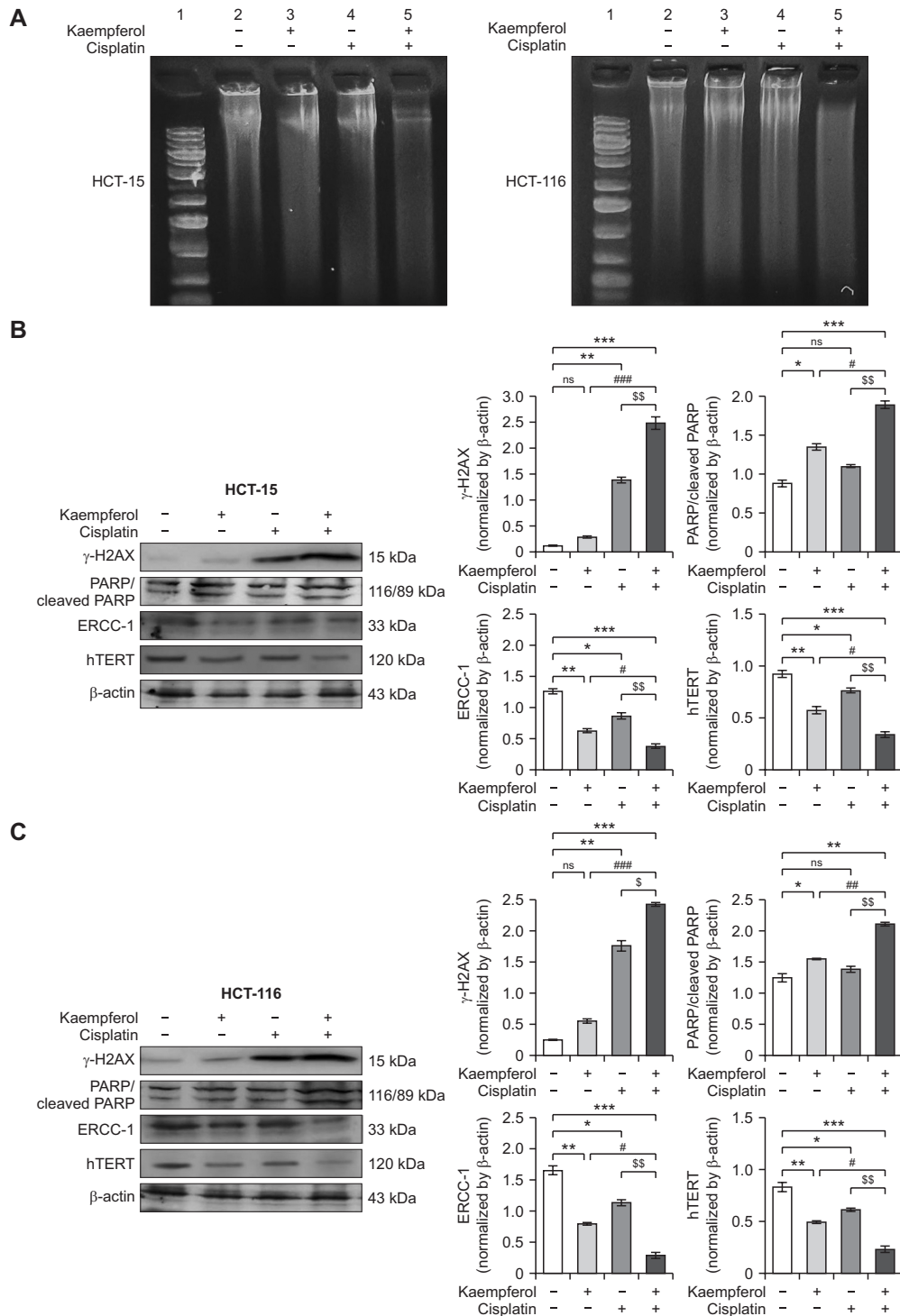


Figure 6. Kaempferol enhances the cisplatin induced DNA damage response in human colon cancer HCT-15 and HCT-116 cells. The colon cancer cells were treated with kaempferol and cisplatin either alone or in combination and the impact of co-treatment was evaluated on the DNA damage by observing the level of DNA fragmentation in DNA gel electrophoresis. (A) DNA of colon cancer cells was visualized on 2% agarose gel. From left to right: Lane 1, DNA marker 1 kb; Lane 2, Control cell's DNA; Lane 3, Kaempferol (50 μ M) treated cells shows DNA fragmentation; Lane 4, Cisplatin (10 μ M) treated cells; and Lane 5, a higher fragmentation was observed in cells co-treated with kaempferol (50 μ M) and cisplatin (10 μ M). (B) HCT-15 and (C) HCT-116; The protein markers involved in DNA damage and repair system were analyzed after treatment with kaempferol and cisplatin or their combination. The relative protein expression intensity was analyzed with ImageJ software. Data are presented as mean \pm standard deviation (SD) from 3 independent experiments. The data are represented as the mean \pm standard deviation. * P < 0.05, ** P < 0.01, and *** P < 0.001 for comparison between control and treated cells, whereas # P < 0.05, ## P < 0.01, and ### P < 0.001 for comparison between kaempferol alone and combination and \$ P < 0.05, \$\$ P < 0.01 for comparison between cisplatin only and combine treatment. ns, not significant.

for HCT-15 and 88% for HCT-116 colon cancer in the control group which was reduced in the treatment groups. The percentage of apoptotic cells was 11.4% and 19.8% for HCT-15 and HCT-116 cells, respectively for the combined treatment group. These results have confirmed the significant impact of the combined treatment of cisplatin and kaempferol on the apoptotic cell death.

Understanding the cellular alterations brought on by the induction of apoptosis can be visualized by DAPI staining, a potent technique for observing nuclear morphology [42]. Our

results demonstrate that co-treatment enhances the results of DAPI staining, leading to a significant modification of nuclear features of apoptosis (Fig. 7B). The AO/EtBr also assessed morphological changes that occur during apoptosis (Figure S2).

The tumor suppressor protein p53, often referred to as TP53 (tumor protein 53), is essential for controlling several cellular functions, such as the progression of the cell cycle, DNA repair, apoptosis, senescence, and metabolism [43]. The combined treatment had a more profound impact on

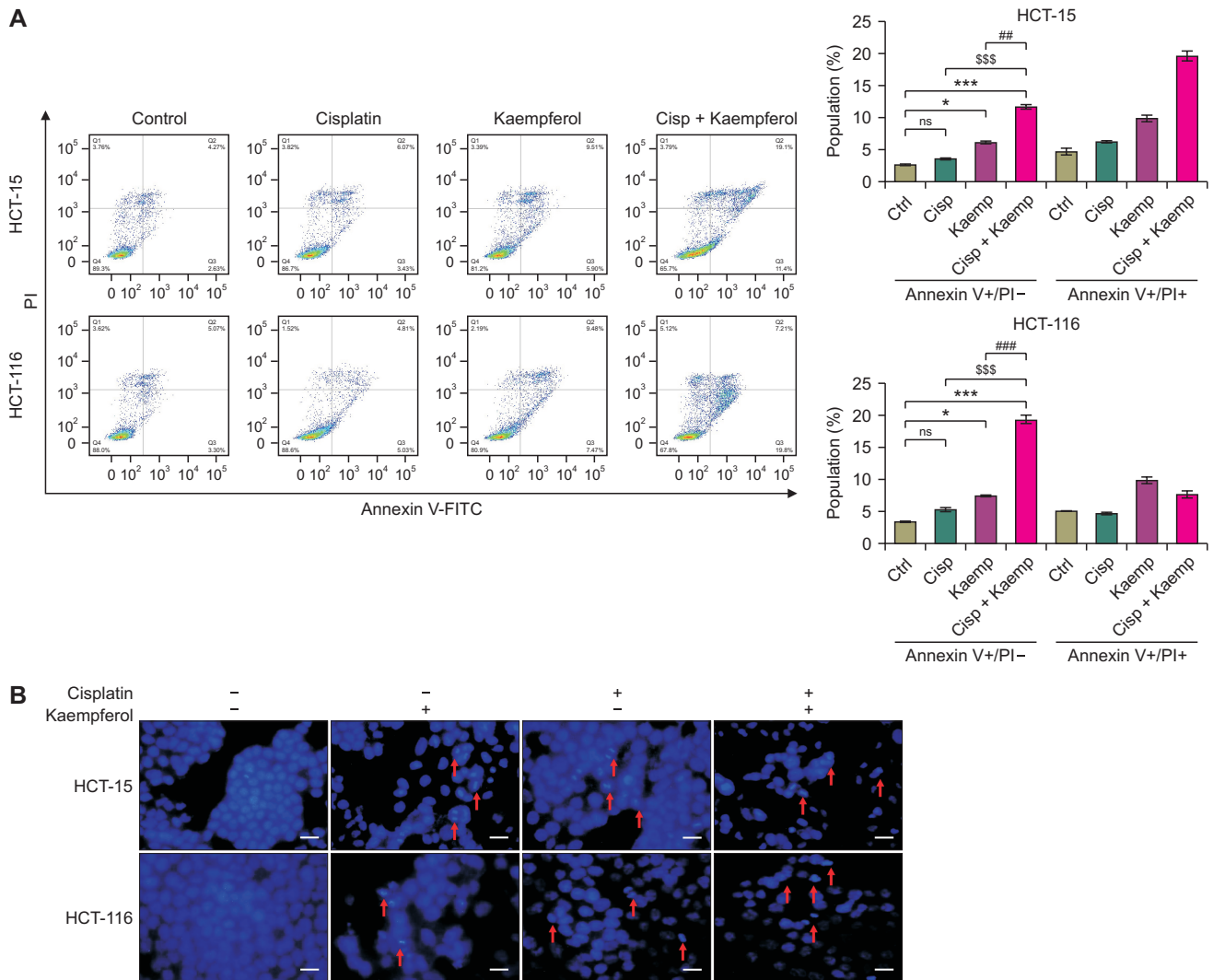
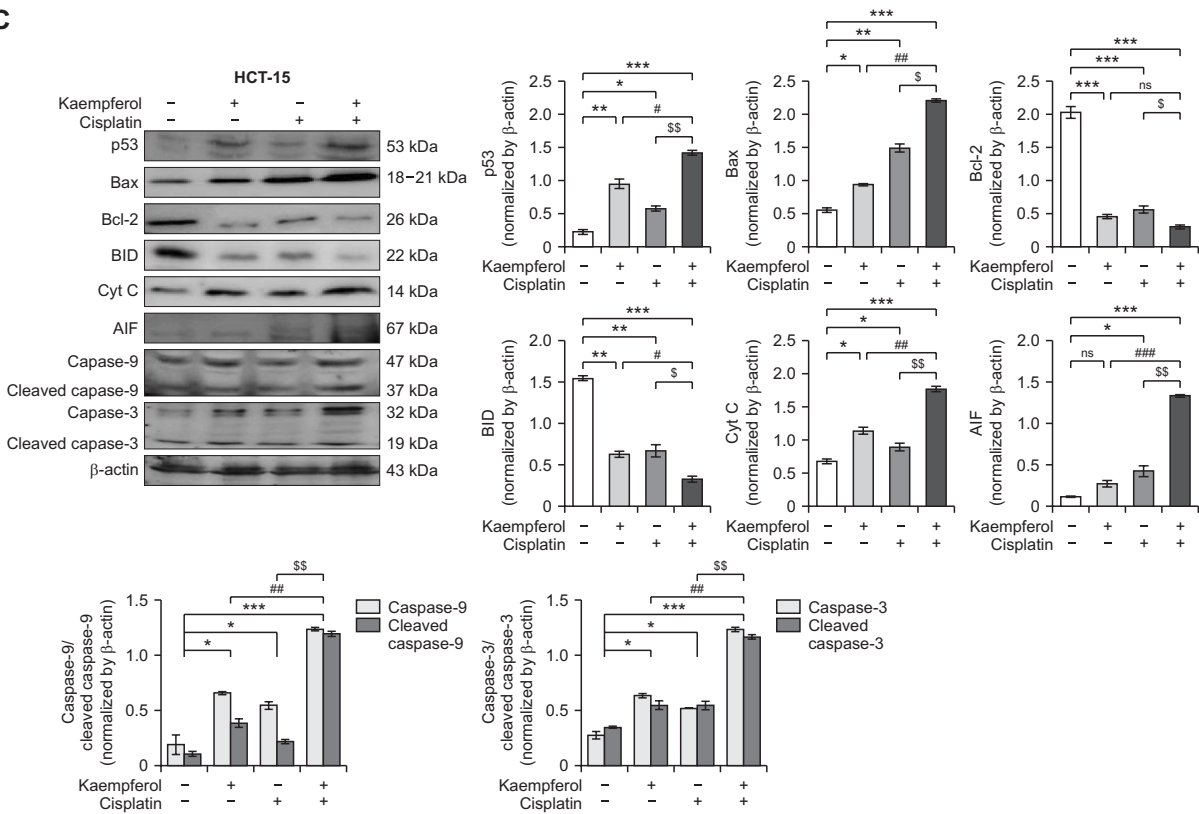


Figure 7. Kaempferol enhances the cisplatin induced apoptotic pathway in colon cancer cells. (A) Apoptosis in colon cancer cells was detected via flow cytometry with Annexin V-FITC and PI staining. Q1-necrosis, Q2-late apoptosis, Q3-early apoptosis, Q4-healthy cells. (B) DNA fragmentation as a sign of apoptosis was confirmed with DAPI staining. HCT-15 and HCT-116 colon cancer cells were treated with kaempferol and cisplatin either alone or in combination for 48 hours and the cell lysates were immunoblotted with relevant antibodies. (C) HCT-15 and (D) HCT-116 cancer cells were checked for apoptosis markers following kaempferol and cisplatin treatment alone or in combination. (E) The functional role of p53 was determined in kaempferol and cisplatin co-treatment in p53-siRNA transfected HCT-116 cells. (F) Cell viability was also assessed in the p53-siRNA transfected group with or without co-treatment of kaempferol and cisplatin. Expression of HSPs were also detected in (G) HCT-15 and (H) HCT-116 cells. Scale bar 100 μ m. The data are represented as the mean \pm standard deviation. * $P < 0.05$, ** $P < 0.01$, and *** $P < 0.001$ for comparison between control and treated cells, whereas # $P < 0.05$, ## $P < 0.01$, and ### $P < 0.001$ for comparison between kaempferol alone and combination and \$\$\$ $P < 0.05$, \$\$\$ $P < 0.01$, and \$\$\$ $P < 0.001$ for comparison between cisplatin only and combine treatment. ns, not significant.

C



D

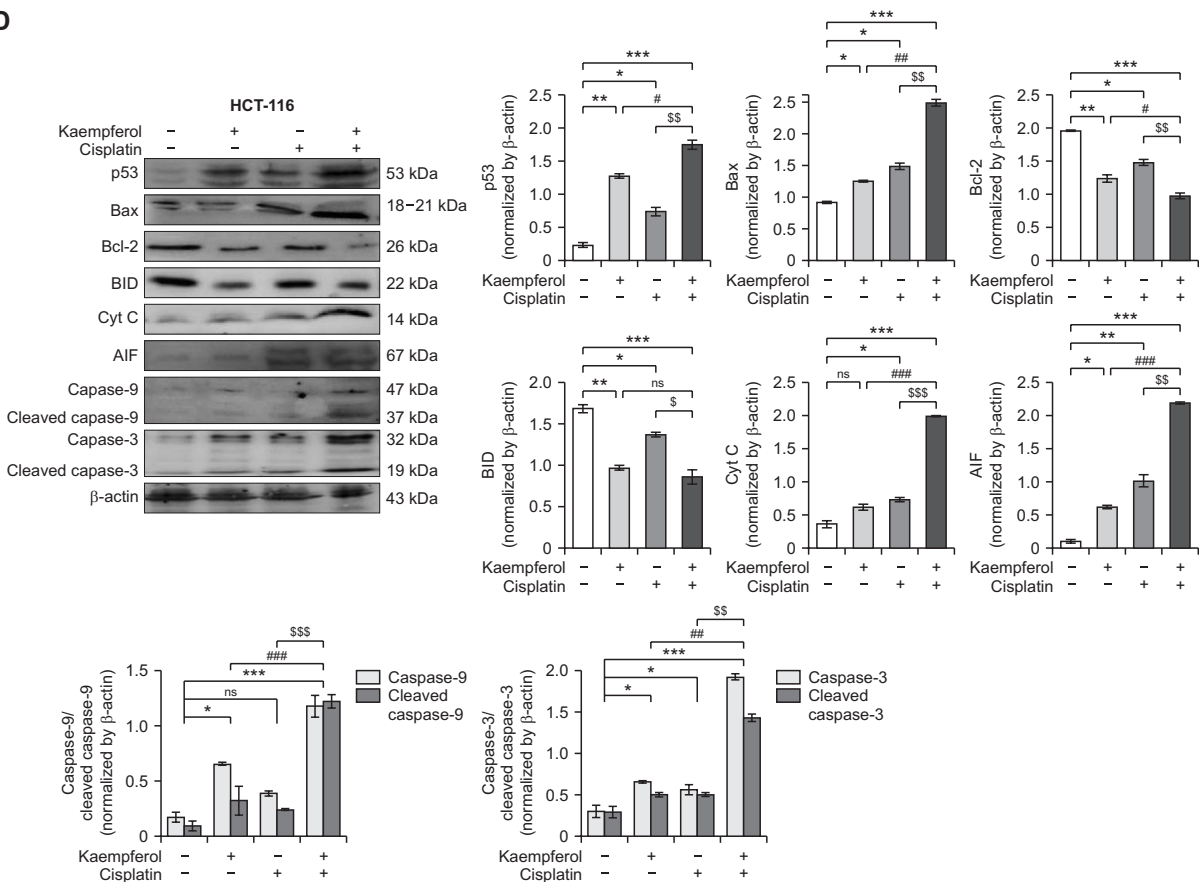


Figure 7. Continued.

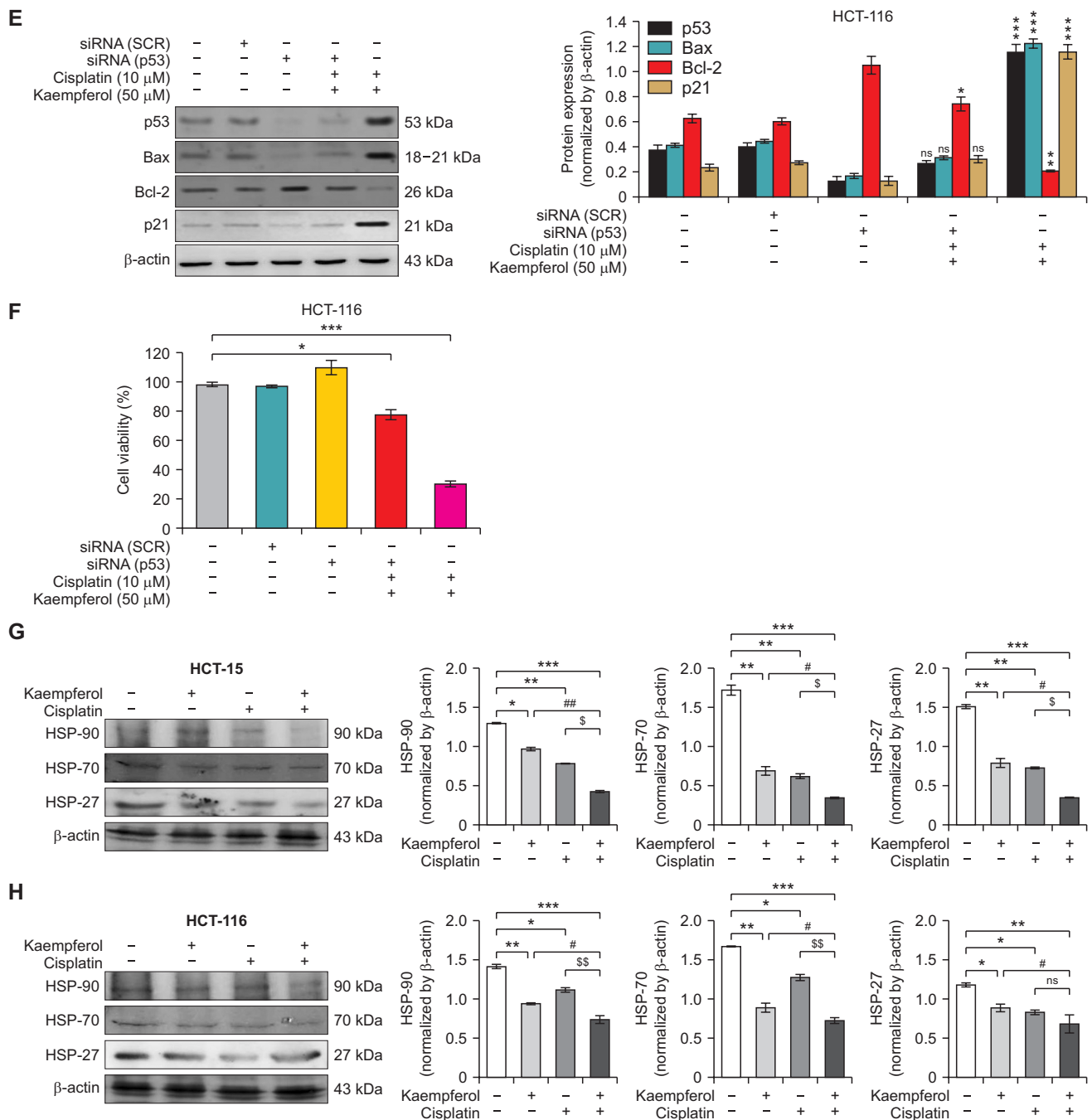


Figure 7. Continued.

the expression of p53 in HCT-15 and HCT-116 cells (Fig. 7C and 7D). To validate the impact on downstream apoptotic pathways, immunoblot analysis was carried out. Proteins belonging to the Bcl-2 family (pro-apoptotic and anti-apoptotic) may bind to the mitochondrial membrane to control the mitochondrial membrane potential change ($\Delta\Psi_m$) in response to apoptotic stimuli [44]. The combined treatment showed a significant increase in the expression of pro-apoptotic proteins such as Bax, apoptosis-inducing factor (AIF), caspase/

cleaved caspase-9 and caspase/cleaved caspase 3 in both HCT-15 and HCT-116 cell lines. In addition, kaempferol and cisplatin co-treatment also significantly increased the cytochrome c protein accumulation. The co-treatment also markedly levels of anti-apoptotic proteins such as Bcl-2 and BID in both cell lines (Fig. 7C and 7D).

To verify the functional role of p53 in the apoptotic response initiated by the co-treatment of kaempferol and cisplatin, we used HCT-116 cells in which p53 expression was

suppressed using p53-siRNA transfection. Western blot analysis revealed the significant reduction of p53 protein levels in cells with p53-siRNA transfection, indicating the successful knockdown of p53 in comparison to control (Fig. 7E). Further protein expression analysis demonstrated changes in the expression patterns of apoptotic markers in cells where p53 was knocked down. More precisely, the levels of pro-apoptotic marker Bax were reduced, while the levels of anti-apoptotic Bcl-2 were increased. Additionally, the expression of the cell cycle regulator p21 was decreased in p53-suppressed HCT-116 cells. Surprisingly, when kaempferol and cisplatin were co-treated together after p53 siRNA transfection, the cells showed improved responses to apoptosis, as evidenced by slight alterations in the expression of markers associated with apoptosis. However, the observed difference was less prominent as compared to cells receiving the same co-treatment without p53 knockdown. Additionally, the MTT assay results showed that cell viability was increased in cells with suppressed p53 expression (Fig. 7F). The p53 knockdown cells receiving the co-treatment had a less significant reduc-

tion in cell viability as compared to the control group while the co-treatment group without p53 knockdown had a significant impact on the reduction of cell viability. The results emphasize the crucial function of p53 in facilitating the apoptotic consequences of combining kaempferol with cisplatin in colon cancer cells.

According to several studies, expression of heat-shock proteins (HSPs) under proteotoxic stress increases cancer cell survival and chemoresistance [45,46]. We thus investigated whether the expression of HSPs was affected by kaempferol and cisplatin treatment either alone or in combination. Our results showed that the kaempferol and cisplatin co-treatment remarkably reduced the levels of HSPs such as HSP-27, HSP-70, and HSP-90 as compared to control (Fig. 7G and 7H). The individual treatment was less effective as compared to the combined treatment.

Kaempferol and cisplatin co-treatment enhanced the cell cycle arrest at G1 phase

Senescent cells have irreversible growth arrest as a key char-

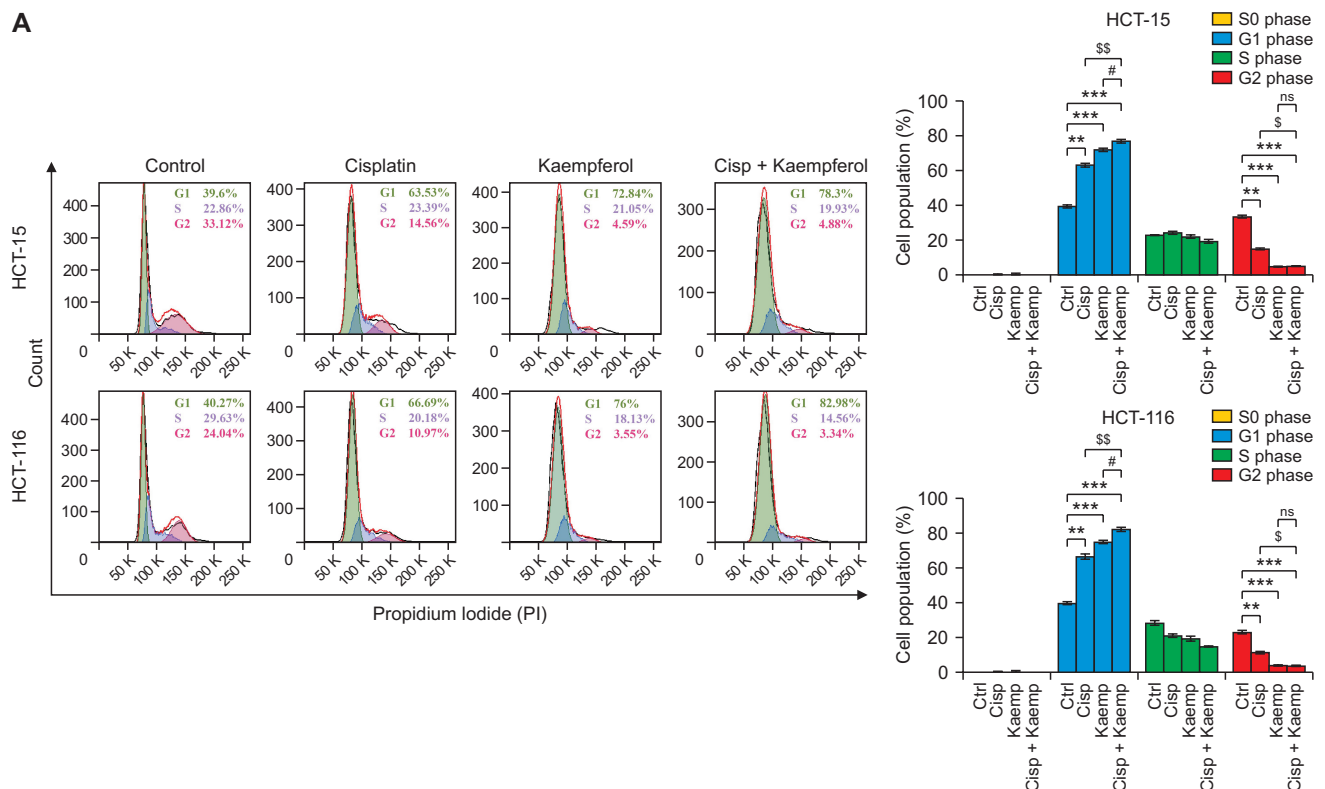


Figure 8. Kaempferol and cisplatin co-treatment induced cell cycle arrest at G1 phase. HCT-15 and HCT-116 colon cancer cells were treated with kaempferol and cisplatin either alone or in combination for 48 hours. (A) The percentage of cell population arrested in G1 phase was analyzed with flow cytometry following the individual or co-treatment. (B) HCT-15 and (C) HCT-116 cancer cells were checked for molecular markers involved in the cell cycle and proliferation normalized with β -actin. (D, E) The cells were analyzed for cyclin-dependent kinase (CDKs) markers which regulates the progression of cells through different cell cycle phases. The relative protein expression of HCT-15 and HCT-116 colon cancer cells was measured with ImageJ software. The data are represented as the mean \pm standard deviation. * $P < 0.05$, ** $P < 0.01$, and *** $P < 0.001$ for comparison between control and treated cells, whereas # $P < 0.05$, ## $P < 0.01$, and ### $P < 0.001$ for comparison between kaempferol alone and combination and \$ $P < 0.05$, \$\$ $P < 0.01$, and \$\$\$ $P < 0.001$ for comparison between cisplatin only and combine treatment. ns, not significant.

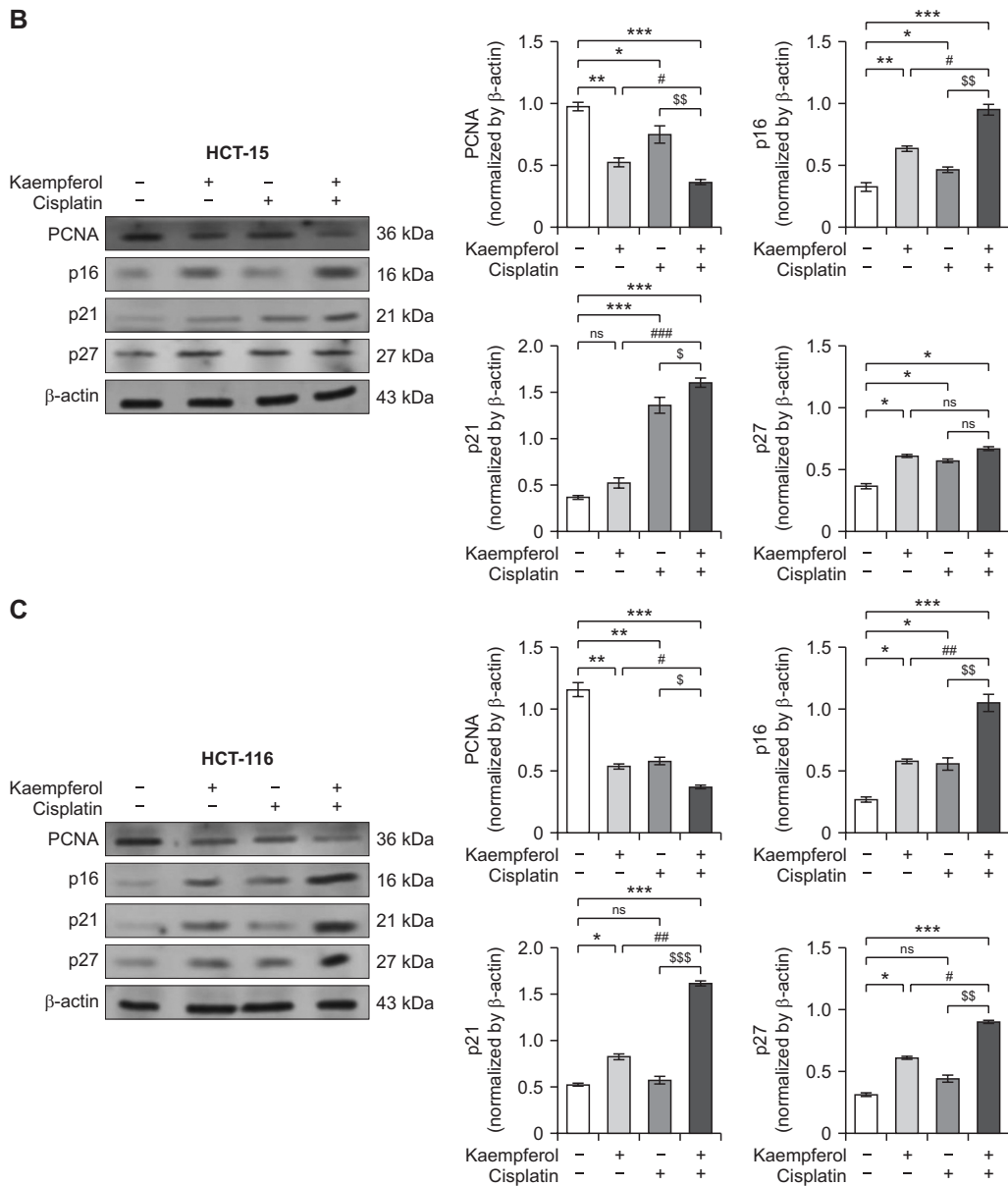


Figure 8. Continued.

acteristic, which occurs when cells acquire sublethal DNA damage and transition into a viable but non-replicating state [47]. To confirm the growth inhibition and cell cycle arrest at the G1 phase, we conducted the cell cycle arrest analysis via flow cytometric detection. As shown in Figure 8A, 78.3% and 82.98% of the cell population were arrested in the G1 phase following cisplatin and kaempferol co-treatment of HCT-15 and HCT-116 cells respectively. The percentage was significantly higher than the control and the individual treatment.

Several molecular pathways are involved in the progression of the cell cycle from one phase to another. Such markers play a key role in surveillance systems that monitor and control the cell's progression to the next phase of the cell cy-

cle [48]. The results showed alterations in the expression pattern of key regulators of the cell cycle (Fig. 8B and 8C). The combination treatment enhanced this impact, demonstrating a notable increase in the expression of p21 and p27 in both cell lines. The increased expression of p21 and p27 is associated with cell cycle arrest at G1 phase because of the inhibition of CDK2 and CDK4/6 [49]. The p21 expression is upregulated in response to p53-mediated DDR [50]. In addition, the levels of p16, another inhibitor of CDKs, were increased after the combined treatment in both cell lines, providing further confirmation of cell cycle arrest. An important protein called proliferating cell nuclear antigen (PCNA) potentiates the efficiency of DNA synthesis in eukaryotic cells by performing

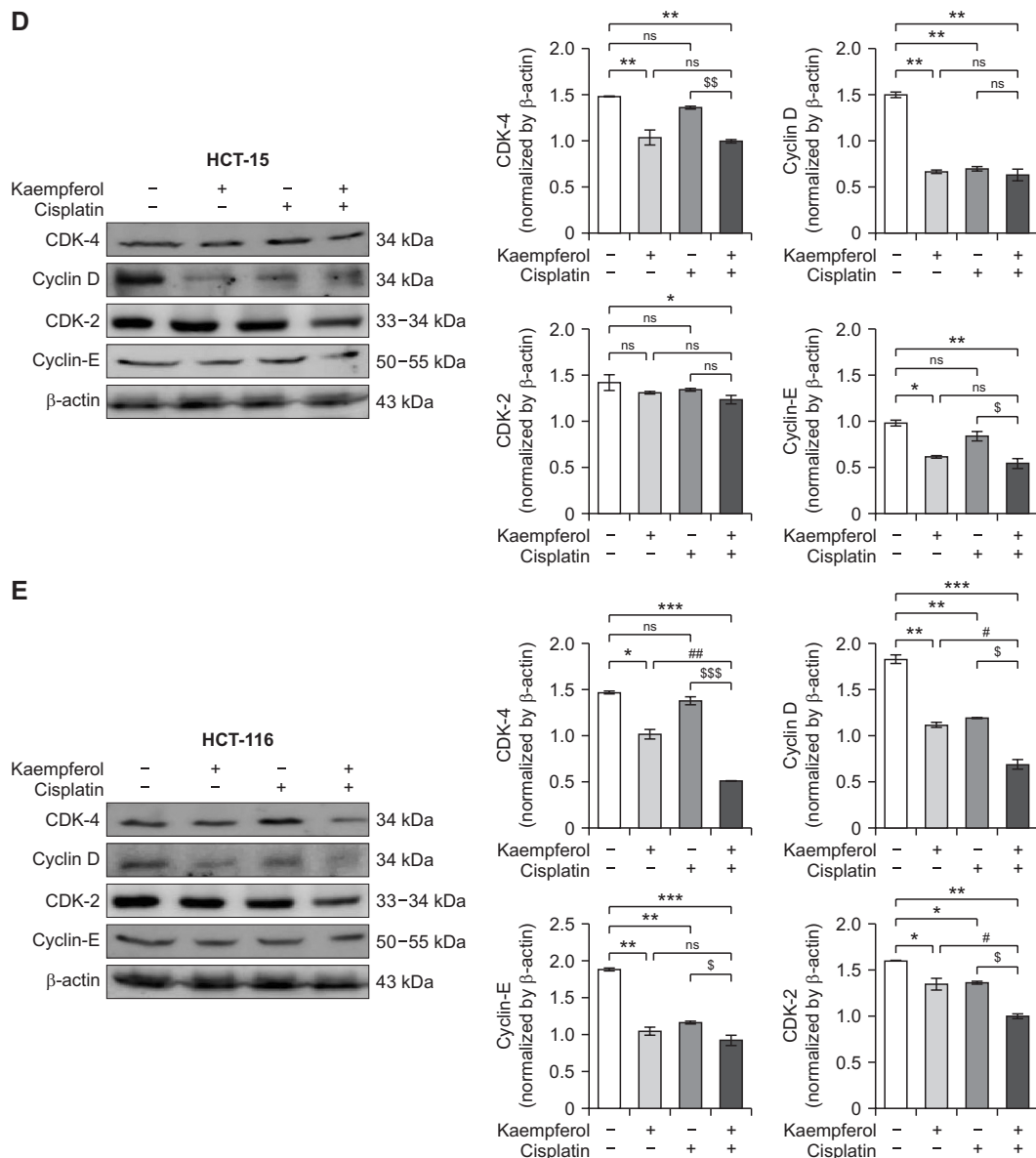


Figure 8. Continued.

as a processivity factor for DNA polymerase δ . It plays an important role in the process of DNA replication and is necessary for the progression of the cell cycle, especially during the S-phase [51]. In our results, the levels of PCNA were significantly decreased in cells that received the kaempferol and cisplatin co-treatment. The results emphasize the increased effectiveness of using both cisplatin and kaempferol together to induce cell cycle arrest in colon cancer cells.

To control cell division through extracellular and intracellular signalling, CDKs, which are catalytic components of cyclins, create a heterodimer complex [52]. We found that kaempferol and cisplatin co-treatment significantly reduced CDKs expression and the associated cyclin complex, which had an impact on cell-cycle progression (Fig. 8D and 8E). Following

the kaempferol and cisplatin co-treatment, the protein expression of CDK-4, Cyclin D, CDK-2, and Cyclin E in HCT-15 was reduced; however, in HCT-116 cells, the co-treatment of kaempferol and cisplatin reduced the expression of CDK-4, Cyclin D, CDK-2 and Cyclin E. These findings collectively showed that co-treatment could prevent cells from moving from the G0/G1 phase to the S phase of the cell cycle.

Our research provides experimental evidence that co-exposure to kaempferol and cisplatin inhibits the proliferation of human colorectal cancer cells. Further, kaempferol increases the process of cisplatin-induced apoptosis in colon cancer cells via several mechanisms such as the reduction of mitochondrial membrane potential, increased oxidative stress, and enhanced DNA damage. The co-treatment significantly

enhances the process of programmed cell death, as evidenced by the altered expression/activation of crucial protein markers associated with apoptosis. We observed a substantial increase in cell cycle arrest at the G1 phase. This indicates the impact of kaempferol on the modulation of cell cycle regulatory proteins while enhancing the effects of cisplatin. Our research offers the justification for using kaempferol as a strong adjuvant option based on molecular investigations. This research promotes the use of kaempferol as a chemotherapeutic adjuvant to conventional anticancer medications to lessen the unfavourable side effects of synthetic toxic chemicals, which may also help prevent the emergence of drug-resistant cancer cells. Additional *in vivo* investigations and clinical evaluations are necessary to confirm the therapeutic efficacy of this combination for the treatment of colon cancer.

FUNDING

This research work was supported by National Research Foundation of Korea grant, NRF RS-2023-00253438.

CONFLICTS OF INTEREST

No potential conflicts of interest were disclosed.

SUPPLEMENTARY MATERIALS

Supplementary materials can be found via <https://doi.org/10.15430/JCP.24.013>.

ORCID

Muhammad Haroon, <https://orcid.org/0009-0006-2509-1238>
Sun Chul Kang, <https://orcid.org/0000-0002-1580-3266>

REFERENCES

- Weng W, Goel A. Curcumin and colorectal cancer: an update and current perspective on this natural medicine. *Semin Cancer Biol* 2022;80:73-86.
- Debela DT, Muzazu SG, Heraro KD, Ndalama MT, Mesele BW, Haile DC, et al. New approaches and procedures for cancer treatment: Current perspectives. *SAGE Open Med* 2021; 9:20503121211034366.
- Bragado P, Armesilla A, Silva A, Porras A. Apoptosis by cisplatin requires p53 mediated p38alpha MAPK activation through ROS generation. *Apoptosis* 2007;12:1733-42.
- Galluzzi L, Vitale I, Michels J, Brenner C, Szabadkai G, Harel-Bellan A, et al. Systems biology of cisplatin resistance: past, present and future. *Cell Death Dis* 2014;5:e1257.
- Wu YL, Zhou C, Hu CP, Feng J, Lu S, Huang Y, et al. Afatinib versus cisplatin plus gemcitabine for first-line treatment of Asian patients with advanced non-small-cell lung cancer harbouring EGFR mutations (LUX-Lung 6): an open-label, randomised phase 3 trial. *Lancet Oncol* 2014;15:213-22.
- Ma Y, Zhang J, Zhang Q, Chen P, Song J, Yu S, et al. Adenosine induces apoptosis in human liver cancer cells through ROS production and mitochondrial dysfunction. *Biochem Biophys Res Commun* 2014;448:8-14.
- Yu L, Liu Z, Qiu L, Hao L, Guo J. Ipatasertib sensitizes colon cancer cells to TRAIL-induced apoptosis through ROS-mediated caspase activation. *Biochem Biophys Res Commun* 2019;519:812-8.
- Xiang T, Du L, Pham P, Zhu B, Jiang S. Nelfinavir, an HIV protease inhibitor, induces apoptosis and cell cycle arrest in human cervical cancer cells via the ROS-dependent mitochondrial pathway. *Cancer Lett* 2015;364:79-88.
- Zou P, Chen M, Ji J, Chen W, Chen X, Ying S, et al. Auranofin induces apoptosis by ROS-mediated ER stress and mitochondrial dysfunction and displayed synergistic lethality with piperlongumine in gastric cancer. *Oncotarget* 2015;6:36505-21.
- Ng CY, Yen H, Hsiao HY, Su SC. Phytochemicals in skin cancer prevention and treatment: an updated review. *Int J Mol Sci* 2018;19:941.
- Georgiev V, Ananga A, Tsoleva V. Recent advances and uses of grape flavonoids as nutraceuticals. *Nutrients* 2014;6:391-415.
- Wang J, Fang X, Ge L, Cao F, Zhao L, Wang Z, et al. Antitumor, antioxidant and anti-inflammatory activities of kaempferol and its corresponding glycosides and the enzymatic preparation of kaempferol. *PLoS One* 2018;13:e0197563.
- Lee J, Kim JH. Kaempferol inhibits pancreatic cancer cell growth and migration through the blockade of EGFR-related pathway *in vitro*. *PLoS One* 2016;11:e0155264.
- Shen CY, Li KJ, Wu CH, Lu CH, Kuo YM, Hsieh SC, et al. Unveiling the molecular basis of inflamm-aging induced by advanced glycation end products (AGEs)-modified human serum albumin (AGE-HSA) in patients with different immune-mediated diseases. *Clin Immunol* 2023;252:109655.
- Dey DK, Chang SN, Kang SC. The inflammation response and risk associated with aflatoxin B1 contamination was minimized by insect peptide CopA3 treatment and act towards the beneficial health outcomes. *Environ Pollut* 2021;268(Pt B):115713.
- He G, He G, Zhou R, Pi Z, Zhu T, Jiang L, et al. Enhancement of cisplatin-induced colon cancer cells apoptosis by shikonin, a natural inducer of ROS *in vitro* and *in vivo*. *Biochem Biophys Res Commun* 2016;469:1075-82.
- Cummings BS, Schnellmann RG. Measurement of cell death in mammalian cells. *Curr Protoc* 2021;1:e210.
- lanevski A, Giri AK, Aittokallio T. SynergyFinder 3.0: an interactive analysis and consensus interpretation of multi-drug synergies across multiple samples. *Nucleic Acids Res* 2022;50(W1):W739-43.
- Huang W, Hickson LJ, Eirin A, Kirkland JL, Lerman LO. Cellular senescence: the good, the bad and the unknown. *Nat Rev Nephrol* 2022;18:611-27.
- Crane AM, Bhattacharya SK. The use of bromodeoxyuridine incorporation assays to assess corneal stem cell proliferation.

- Methods Mol Biol 2013;1014:65-70.
21. Valieva Y, Ivanova E, Fayzullin A, Kurkov A, Igrunkova A. Senescence-associated β -galactosidase detection in pathology. *Diagnostics (Basel)* 2022;12:2309.
 22. Scholzen T, Gerdes J. The Ki-67 protein: from the known and the unknown. *J Cell Physiol* 2000;182:311-22.
 23. 24. Maryanovich M, Gross A. A ROS rheostat for cell fate regulation. *Trends Cell Biol* 2013;23:129-34.
 24. Drew B, Leeuwenburgh C. Aging and the role of reactive nitrogen species. *Ann N Y Acad Sci* 2002;959:66-81.
 25. Hsieh HJ, Liu CA, Huang B, Tseng AH, Wang DL. Shear-induced endothelial mechanotransduction: the interplay between reactive oxygen species (ROS) and nitric oxide (NO) and the pathophysiological implications. *J Biomed Sci* 2014;21:3.
 26. Ju H, Pachhapure S, Mufida A, Kim A, Elmaleh DR, Choi S, et al. 2-aryl propionic acid amide modification of naproxen and ibuprofen dimers for anti-neuroinflammatory activity in BV2 mouse microglial cells. *Keimyung Med J* 2022;41:56-66.
 27. Shang D, Hong Y, Xie W, Tu Z, Xu J. Interleukin- β drives cellular senescence of rat astrocytes induced by oligomerized amyloid β peptide and oxidative stress. *Front Neurol* 2020;11:929.
 28. Lee KM, Lee KW, Jung SK, Lee EJ, Heo YS, Bode AM, et al. Kaempferol inhibits UVB-induced COX-2 expression by suppressing Src kinase activity. *Biochem Pharmacol* 2010;80:2042-9.
 29. Espinosa-Diez C, Miguel V, Mennerich D, Kietzmann T, Sánchez-Pérez P, Cadenas S, et al. Antioxidant responses and cellular adjustments to oxidative stress. *Redox Biol* 2015;6:183-97.
 30. Guo C, Sun L, Chen X, Zhang D. Oxidative stress, mitochondrial damage and neurodegenerative diseases. *Neural Regen Res* 2013;8:2003-14.
 31. Zorova LD, Popkov VA, Plotnikov EY, Silachev DN, Pevzner IB, Jankauskas SS, et al. Mitochondrial membrane potential. *Anal Biochem* 2018;552:50-9.
 32. Yang Y, An Y, Ren M, Wang H, Bai J, Du W, et al. The mechanisms of action of mitochondrial targeting agents in cancer: inhibiting oxidative phosphorylation and inducing apoptosis. *Front Pharmacol* 2023;14:1243613.
 33. Choi SG, Shin M, Kim WY. Targeting the DNA damage response (DDR) of cancer cells with natural compounds derived from *Panax ginseng* and other plants [published online ahead of print April 9, 2024]. *J Ginseng Res*. doi: 10.1016/j.jgr.2024.04.001
 34. Shadfar S, Parakh S, Jamali MS, Atkin JD. Redox dysregulation as a driver for DNA damage and its relationship to neurodegenerative diseases. *Transl Neurodegener* 2023;12:18.
 35. Samarghandian S, Shabestari MM. DNA fragmentation and apoptosis induced by safranal in human prostate cancer cell line. *Indian J Urol* 2013;29:177-83.
 36. Podhorecka M, Skladanowski A, Bozko P. H2AX Phosphorylation: its role in DNA damage response and cancer therapy. *J Nucleic Acids* 2010;2010:920161.
 37. Firsanov DV, Solovjeva LV, Svetlova MP. H2AX phosphorylation at the sites of DNA double-strand breaks in cultivated mammalian cells and tissues. *Clin Epigenetics* 2011;2:283-97.
 38. Kuo LJ, Yang LX. Gamma-H2AX - a novel biomarker for DNA double-strand breaks. *In Vivo* 2008;22:305-9.
 39. McNeil EM, Melton DW. DNA repair endonuclease ERCC1-XPF as a novel therapeutic target to overcome chemoresistance in cancer therapy. *Nucleic Acids Res* 2012;40:9990-10004.
 40. Liu Y, Betori RC, Pagacz J, Frost GB, Efimova EV, Wu D, et al. Targeting telomerase reverse transcriptase with the covalent inhibitor NU-1 confers immunogenic radiation sensitization. *Cell Chem Biol* 2022;29:1517-31.e7.
 41. Fan HC, Chang FW, Tsai JD, Lin KM, Chen CM, Lin SZ, et al. Telomeres and Cancer. *Life* 2021;11:1405.
 42. Wlodkovic D, Telford W, Skommer J, Darzynkiewicz Z. Apoptosis and beyond: cytometry in studies of programmed cell death. *Methods Cell Biol* 2011;103:55-98.
 43. Li W, Du B, Wang T, Wang S, Zhang J. Kaempferol induces apoptosis in human HCT116 colon cancer cells via the Ataxia-Telangiectasia Mutated-p53 pathway with the involvement of p53 upregulated modulator of apoptosis. *Chem Biol Interact* 2009;177:121-7.
 44. Cory S, Adams JM. The Bcl2 family: regulators of the cellular life-or-death switch. *Nat Rev Cancer* 2002;2:647-56.
 45. Dai C, Whitesell L, Rogers AB, Lindquist S. Heat shock factor 1 is a powerful multifaceted modifier of carcinogenesis. *Cell* 2007;130:1005-18.
 46. Zou J, Guo Y, Guettouche T, Smith DF, Voellmy R. Repression of heat shock transcription factor HSF1 activation by HSP90 (HSP90 complex) that forms a stress-sensitive complex with HSF1. *Cell* 1998;94:471-80.
 47. Herranz N, Gil J. Mechanisms and functions of cellular senescence. *J Clin Invest* 2018;128:1238-46.
 48. Malumbres M. 4 - Control of the Cell Cycle. 6th edition. Abeloff's Clinical Oncology, pp 56-73.e5, 2020.
 49. Pandey K, Park N, Park KS, Hur J, Cho YB, Kang M, et al. Combined CDK2 and CDK4/6 inhibition overcomes palbociclib resistance in breast cancer by enhancing senescence. *Cancers (Basel)* 2020;12:3566.
 50. Al Bitar S, Gali-Muhtasib H. The role of the cyclin dependent kinase inhibitor p21cip1/waf1 in targeting cancer: molecular mechanisms and novel therapeutics. *Cancers (Basel)* 2019;11:1475.
 51. Strzalka W, Ziemienowicz A. Proliferating cell nuclear antigen (PCNA): a key factor in DNA replication and cell cycle regulation. *Ann Bot* 2011;107:1127-40.
 52. Ding L, Cao J, Lin W, Chen H, Xiong X, Ao H, et al. The roles of cyclin-dependent kinases in cell-cycle progression and therapeutic strategies in human breast cancer. *Int J Mol Sci* 2020;21:1960.